Electrophysiological analyses of transgenic mice overexpressing KCNJ8 with S422L mutation in cardiomyocytes

Watanabe, Yasuhiro ; Matsumoto, Akio ; Miki, Takashi ; Seino, Susumu ; Anzai, Naohiko ; Nakaya, Haruaki

(Citation)
Journal of Pharmacological Sciences,135(1):37-43

(Issue Date)
2017-09

(Resource Type)
journal article

(Version)
Version of Record

(URL)
https://hdl.handle.net/20.500.14094/90004537

Journal of Pharmacological Sciences 135 (2017) 37–43

Contents lists available at ScienceDirect

Journal of Pharmacological Sciences

journal homepage: www.elsevier.com/locate/jphs

Full paper

Electrophysiological analyses of transgenic mice overexpressing *KCNJ8* with S422L mutation in cardiomyocytes☆

Yasuhiro Watanabe [a], Akio Matsumoto [a], Takashi Miki [b], Susumu Seino [c], Naohiko Anzai [a], Haruaki Nakaya [a, *]

[a] Department of Pharmacology, Chiba University Graduate School of Medicine, Chuo-ku, Chiba 260-8670, Japan
[b] Department of Medical Physiology, Chiba University Graduate School of Medicine, Chuo-ku, Chiba 260-8670, Japan
[c] Division of Molecular and Metabolic Medicine, Kobe University Graduate School of Medicine, Chuo-ku, Kobe 650-0017, Japan

ARTICLE INFO

Article history:
Received 5 June 2017
Received in revised form
26 July 2017
Accepted 17 August 2017
Available online 6 September 2017

Keywords:
K_{ATP} channel
J wave syndrome
KCNJ8 (Kir6.1)-S422L mutation
Transgenic mouse
Patch-clamp techniques

ABSTRACT

Genetic analysis of *KCNJ8* has pointed a mutation (S422L) as a susceptible link to J wave syndrome (JWS). *In vitro* expression study indicated that the ATP-sensitive K^+ (K_{ATP}) channel with the S422L mutation has the gain-of-function with reduced sensitivity to ATP. However, the electrophysiological impact of *KCNJ8* has not been elucidated *in vivo*. Transgenic mouse strains overexpressing *KCNJ8* S422L variant (TGmt) or WT (TGWT) in cardiomyocytes have been created to investigate the influence of *KCNJ8* in cardiomyocytes and the JWS-related feature of the S422L variant on the cardiac electrophysiology. These TG strains demonstrated distinct changes in the J-ST segment of ECG with marked QT prolongation, which might be ascribed to the action potential prolongation resulting from the reduction of voltage-dependent K^+ currents in ventricular cells. The pinacidil-induced K_{ATP} current was decreased in these TG myocytes and no obvious difference between TG and non-TG (WT) myocytes in the ATP sensitivity of the K_{ATP} channel was observed although the open probability of the K_{ATP} channels was significantly lower in TG myocytes than WT. These transgenic mouse strains with distinct ECG changes suggested that the S422L mutation in *KCNJ8* gene is not a direct cause of JWS.

1. Introduction

Early repolarization (ER) patterns in electrocardiogram (ECG), often characterized by a “notch” or “slur” at the J point, have gained increasing attention because of its association with recurrent ventricular fibrillation.[1] Although ER pattern in ECG has been considered as a benign manifestation commonly seen in healthy young males or athletes, several lines of evidence have suggested ER patterns sporadically predict lethal ventricular arrhythmias associated with J wave syndrome (JWS) including ER syndrome (ERS) and Brugada syndrome (BrS).[2]

Emerging evidence indicates that the pathogenesis of JWS partly associates with a genetic variant of *KCNJ8* (Kir6.1) gene, encoding a pore-forming subunit of ATP-sensitive potassium (K_{ATP}) channel.[3] A missense mutation of serine at position 422 in Kir6.1 to leucine (S422L) has been disclosed in association with ERS.[4] Heterologous expression of Kir6.1 and SUR2A in cultured cells extrapolated that S422L mutation can augment K_{ATP} channel activity due to the reduced sensitivity to intracellular ATP.[5,6] Thus, the causal link between JWS and the gain-of-function mutation (S422L) in Kir6.1 has been proposed.

The K_{ATP} channel was identified in cardiomyocytes as a regulator of cellular energy metabolism in the control of membrane excitability.[7] The K_{ATP} channel is a hetero-octameric protein of four pore-forming Kir6.x and four sulfonylurea receptor (SUR) subunits.[7] The sarcolemmal K_{ATP} channels in ventricular myocytes are composed primarily of Kir6.2 and SUR2A subunits whereas K_{ATP} channels in vascular smooth muscle cells are composed primarily of Kir6.1 and SUR2B. Kir6.1 subunit plays a critical role in the regulation of vascular contractility[7]; however, little is known about

☆ **Grant**: This work was partly supported by JSPS KAKENHI Grant Numbers 26460334 and 26670119.

* Corresponding author. Department of Pharmacology, Chiba University Graduate School of Medicine, 1-8-1 Inohana Chuo-ku, Chiba 260-8670, Japan. Fax: +81 43 226 2052.
E-mail address: nakaya@faculty.chiba-u.jp (H. Nakaya).

Peer review under responsibility of Japanese Pharmacological Society.

http://dx.doi.org/10.1016/j.jphs.2017.08.009

the physiological role of Kir6.1 in the K_{ATP} channel activities in cardiomyocytes.

We hence focused on the Kir6.1 in cardiomyocytes to test the hypothesis whether the Kir6.1-S422L mutation can be a direct cause of JWS *in vivo*. We created Kir6.1 transgenic (TG) mouse strains overexpressing S422L mutant (TGmt) or wild-type (TGWT) in cardiomyocytes, respectively, to investigate the potential impact on the cardiac electrophysiology. Electrophysiological data, obtained from this study, did not support the hypothesis that Kir6.1-S422L mutation is a direct cause of JWS.

2. Materials and methods

2.1. Kir6.1 transgenic mice

A fusion gene comprising promoter region of the mouse alpha myosin heavy chain gene (generous gift by Dr. J. Gulick)[8] and rat *KCNJ8* (Kir6.1) cDNA coding sequences[9] was cloned into pBlueScriptII-SK(+) plasmid. The S422L mutation in *KCNJ8* was introduced by PCR with the primer set, Kir6.1HumRat-S422L (Table 1) using PrimeSTAR HS DNA polymerase (Takara Bio, Shiga). Since the S422L mutation was identified from the human subjects and closely locates to the C-terminal, two additional mutations (C420N and P421T) were introduced to humanize the surrounding amino acids, resulting in the amino acid sequence (396–424) identical to human *KCNJ8*. This construct was termed as the humanized S422L mutant. Plasmids for *KCNJ8* wild-type and humanized S422L mutant were confirmed by DNA sequencing. The alpha-MHC-Kir6.1 cassette was micro-injected into the pronucleus of fertilized C57BL/6NCrSlc mice (SLC, Shizuoka) eggs. Transgenic (TG) mice were identified by PCR of tail DNA with the primer set, aMHC-1fw and Kir6.1-3rc. At least two lines of transgenic mouse strains for each *KCNJ8* transgene were selected for the experiments.

Transgenic mice were used as heterozygotes, and bred at the animal facility of Chiba University. Animals were maintained on standard mouse food on a 12-h light/12-h dark cycle. All experimental procedures were approved by the animal research committee of Chiba University. All data were obtained from 10 to 20-wk-old male and female TG mice and age-matched non-transgenic C57BL/6 mice were used as control mice.

2.2. Gene expression analysis in the heart

Gene expression levels were analyzed by semi-quantitative real-time PCR. Mouse heart was quickly removed after sacrifice, stored in RNA*later* Stabilization Solution (Ambion, Austin, TX, USA) at −80 °C until use. Ventricular tissue was sampled in RNA*later* under the stereomicroscope, and total RNA was extracted with RNAiso PLUS (Takara Bio, Shiga). Two μg of total RNA was then used to synthesize first strand cDNA with a SuperScript VILO cDNA Synthesis Kit (Invitrogen, Carlsbad, CA, USA). mRNA levels were quantified by real-time PCR with SYBR green dye (Toyobo, Osaka) with the specific primer sets shown in Table 1, and normalized to ribosomal protein L4 (RPL4) mRNA.[10] Gene expression levels of *KCNJ8* in ventricular tissues from TG mouse strains were in the range of 230–430-fold higher than those from WT littermates (data not shown).

Table 1
Primer sets used for PCR.

Primer name	Sequence (5′ − 3′)
Kir6.1HumRat-S422L.For	AAACCAGAATACTCTAGAATCATGAGGGCAGGAT
Kir6.1HumRat-S422L.Rev	ATGATTCTAGAGTATTCTGGTTTCCTTCTGGAGT
Kir6.1rRT.For	AAGGCATCACGGAGAAGAGT
Kir6.1rRT.Rev	GAGAAACGCAGAAGTGAATGAC
Kir6.2mRT.For	AAGGCCAAGCCCAAGTTTA
Kir6.2mRT.Rev	CCACCACTCTACATACCATACTTCAC
SUR1mRTnew.For	CTTCAGCGGCACCATCAGA
SUR1mRTnew.Rev	TCCAGAGCCTCCCAGAGTGT
SUR2mRT.For	GGAGTGTGATACTGGTCCAA
SUR2mRT.Rev	ACCAGGTCTGCAGTCAGAAT
RPL4.MouseNew.For	GCCAAGACTATGCGCAGGAAT
RPL4.MouseNew.Rev	GTAGCTGCTGCTTCCAGCTT

2.3. Surface ECG recordings and blood pressure measurements

Mouse was anesthetized with a combination of midazolam (Astellas Pharma, Tokyo, 4 mg/kg), butorphanol (Meiji Seika Pharma, Tokyo, 5 mg/kg), and medetomidine (Nippon Zenyaku Kogyo, Fukushima, 0.3 mg/kg). Surface ECG recordings were performed on the temperature-controlled table. Since the diagnostic J wave of the human appears on a precordial lead,[2] we recorded a precordial lead at the left anterior axillary line (V5) along with standard limb leads and analyzed V5 lead ECG. Noninvasive blood pressure (BP) measurement was performed by tail-cuff plethysmography (Softron Inc., Tokyo) in conscious mice.

2.4. Isolation of ventricular cardiomyocytes

Anesthetized mouse was anticoagulated with heparin-Na (Mochida Pharmaceutical, Tokyo, 100 U/kg, i.v.). Heart was quickly excised and Langendorff-perfused with oxygenated HEPES-Tyrode solution (pH 7.4).[11] The ventricular myocytes were enzymatically-isolated and stored in modified Kraft-Brühe solution.

2.5. Patch-clamp experiments

The whole cell patch-clamp techniques were used for the electrical recordings of the action potential (AP), voltage-dependent K^+ currents, and the pinacidil-induced K_{ATP} current at 37 °C.

Action potential was recorded in a current-clamp mode, and the voltage-dependent K^+ currents were recorded in a voltage-clamp mode. Whole cell currents were normalized as current density by cell capacitance. The pinacidil-induced K_{ATP} current was recorded in a voltage-clamp mode, using a ramp pulse protocol to obtain the quasi-steady-state membrane current. The pipette solution contained less ATP (1 mM, pH 7.4). A patch-clamp amplifier (CEZ-2400, Nihon Kohden, Tokyo) was used and the current signals were digitized (Digidata 1322A, Axon Instruments Inc., Union City, CA, USA) at 2 kHz and stored on a computer for later analysis with pCLAMP9 software (Axon Instruments).

Single K_{ATP} channel activity was recorded in the open cell-attached patches of the ventricular cells at room temperature, as previously described.[12] The unitary K_{ATP} current was recorded as outward current with the glass pipette held inside at +40 mV. Single channel data were also analyzed with pCLAMP9 software.

2.6. Materials and reagents

All materials were from Wako Pure Chemical Industries (Osaka) unless otherwise indicated. The following chemicals were purchased from Sigma–Aldrich (St. Louis, MO, USA); Pinacidil monohydrate (P154), glibenclamide (G0639), adenosine 5′-triphosphate dipotassium salt (A8937), and EGTA (E4378). Creatine phosphate dipotassium salt (237911) was purchased from Calbiochem (La Jolla, CA, USA).

2.7. Data analysis

All data were expressed as mean ± SEM unless otherwise indicated. Statistical analysis of the data was performed with Prism software (Ver. 6, GraphPad Software, La Jolla, CA, USA) using one-

way ANOVA with post-hoc Tukey HSD test. A p-value less than 0.05 was considered to be statistically significant.

3. Results

3.1. Creation of KCNJ8 (Kir6.1) transgenic mouse strains

Following selection of founder mice in each transgene strain, founder mice were backcrossed to the parental C57BL/6 strain at least five generations to decrease the passenger gene effect[13] prior to the experimental use. We named TG strains expressing *KCNJ8* wild-type gene as TGWT (Line 634, 673), and TG strains expressing *KCNJ8* gene with humanized S422L mutation as TGmt (Line 105, 111). These TG mice grew normally and there were few unexpected sudden deaths observed until 20 weeks after birth.

We referred the systemic blood pressure since vascular K_{ATP} channel is composed of Kir6.1.[7] There was no significant difference in blood pressure among WT and TG strains (WT: 106 ± 3/69 ± 2, TGmt: 100 ± 2/66 ± 2, and TGWT: 105 ± 2/69 ± 2 mmHg of systolic/diastolic blood pressure, 12–14 mice in each group).

3.2. Atypical ECG changes in TG mice

Electric activity of the heart was monitored by standard surface ECG recordings. In general, mouse ECG presents J point elevation as a notch followed by an inverted T wave, which is in analogous to human J wave pattern (Fig. 1A WT).[14] The J point and the ST segment were the dominant targets among the Kir6.1 transgenic mice. Distinct patterns in the J-ST segment were characterized in two categories; one as enlarged J wave and the other is J-ST segment depression (Fig. 1A TGmt and TGWT). There were few observations in TG strains with normal ECG pattern similar to WT; however, ECG records from Line 673 (TGWT) were relatively similar to WT among TG strains.

Further analyses of ECG records revealed that QT intervals from all TG strains, as well as QTc intervals, were significantly (about 60–100%) longer than WT (Fig. 1B). QT/QTc intervals from Line 673 (TGWT), whose ECG relatively resembled WT among the TG strains, were significantly shorter than other TG lines, although it was still 60% longer than WT.

3.3. Membrane potentials recorded from ventricular myocytes

Since surface ECG recordings from TGmt and TGWT showed atypical patterns on the J-ST segment, we applied the patch-clamp techniques to reveal electrophysiological changes in a ventricular myocyte from these TG mice. Action potentials were recorded in a current-clamp mode (Fig. 2A). APD at 90% repolarization level (APD_{90}) was about 100–200% longer in TG ventricular cells than WT cells (Fig. 2B). These findings are in line with the prolonged QT intervals recorded in surface ECG. However, there was no significant difference in APD_{90} between TGmt and TGWT.

3.4. Membrane currents in ventricular myocytes

Since APD prolongation was remarkable in TG myocyte, we measured membrane currents. First in series, we focused on the voltage-dependent K^+ currents such as the transient outward current (I_{to}), the delayed rectifier K^+ current (I_K), and the inward rectifier K^+ current (I_{K1}). Representative recordings of I_{to} and I_{K1} are

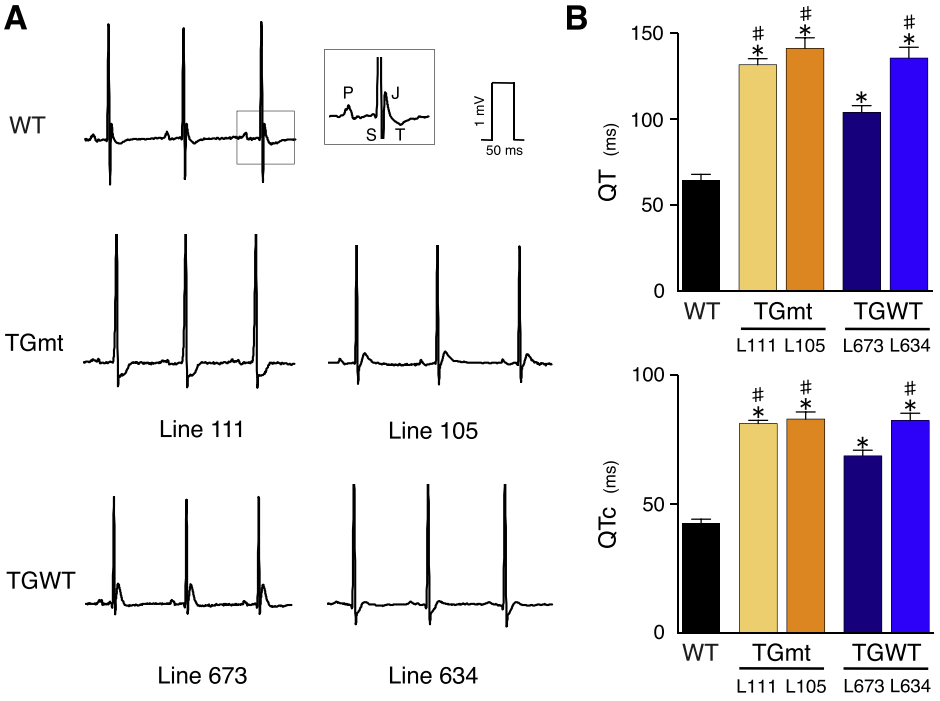

Fig. 1. Representative surface ECG recorded from WT and TG mice. A: Characteristic changes in the J-ST segment in Kir6.1 TG mice. Mouse ECG normally has a notch (J wave) after the QRS complex with the inverted T wave (enlarged view in the inset). The J-ST segment is the point where Kir6.1 TG mice represent characteristic changes, such as an enlarged J wave or J-ST segment depression. Enlarged J wave was defined when the ratio of J wave area to QRS area was greater than 0.25. J-ST segment depression was ECG change with J point depression more than 0.1 mV. J-ST segment depression was the major form in Line 111 (TGmt) (92%) and Line 634 (TGWT) (95%), although 30% of Line 105 (TGmt) and 81% of Line 673 (TGWT) showed enlarged J wave rather than J-ST depression. No spontaneous interconversion between these patterns was observed in the subject. There were few mice in TG strains showing WT pattern. **B:** QT prolongation in TG mouse strains. QT and QTc interval, calculated using Mitchell's formula ($QTc = QT/(RR/100)^{1/2}$), were longer by about 60–100% in both TG strains compared with WT. Among the four TG lines, Line 673 showed shortest QT/QTc intervals. These strains showed sinus rhythm, and there were no significant differences in heart rate and PQ interval. N = 8–21 (mice) in each group. Data are presented as mean ± SEM. $^*p < 0.01$ vs. WT, $\#p < 0.01$ vs. Line 673, respectively.

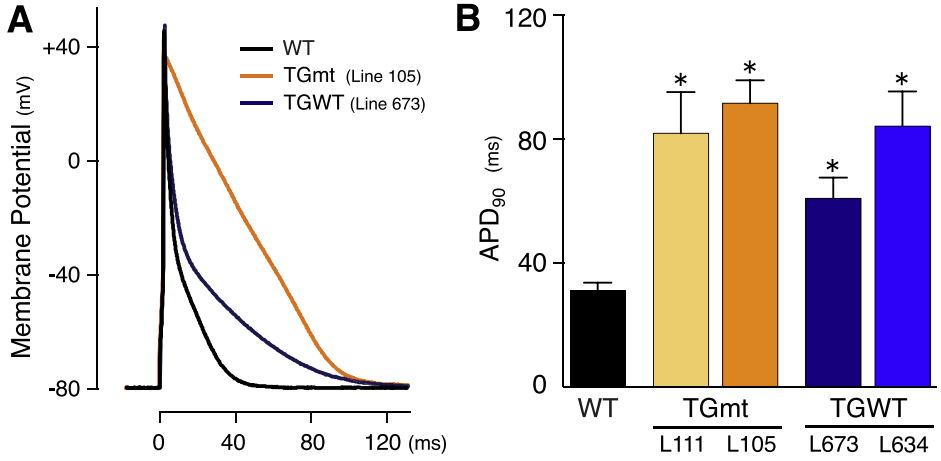

Fig. 2. APD prolongation in ventricular cells of Kir6.1 TG mouse strains. A: Action potentials recorded from cardiomyocytes of WT and TG strains at an interval of 5 s. APD (action potential duration) was markedly prolonged in TGmt (Line 105) and TGWT (Line 673) strains. **B:** APD_{90} (APD_{90} at the 90% repolarization level) measured from WT and TG ventricular cells. APD_{90} was about 100–200% longer in TG ventricular cells compared with WT. There were no significant differences between TGmt and TGWT in APD_{90}. No difference was observed in the resting membrane potential and the phase-0 amplitude among ventricular cells of all experimental groups. N = 11–30 (cells) in each group. Data are expressed as mean ± SEM. $^*p < 0.01$ vs. WT.

shown in Fig. 3A. It was obvious that ventricular cells from TG mouse had less I_{to} than WT ventricular cells. Fig. 3B summarizes the I_{to}, I_K, and I_{K1} densities normalized by membrane capacitance. Overall, TG myocytes had less K^+ current densities compared with WT. Although there were no significant differences in I_{to}, I_K, and I_{K1} densities among the ventricular cells of four TG lines, ventricular cells of Line 673 (TGWT) had comparatively large current densities especially in I_{to} and I_{K1}.

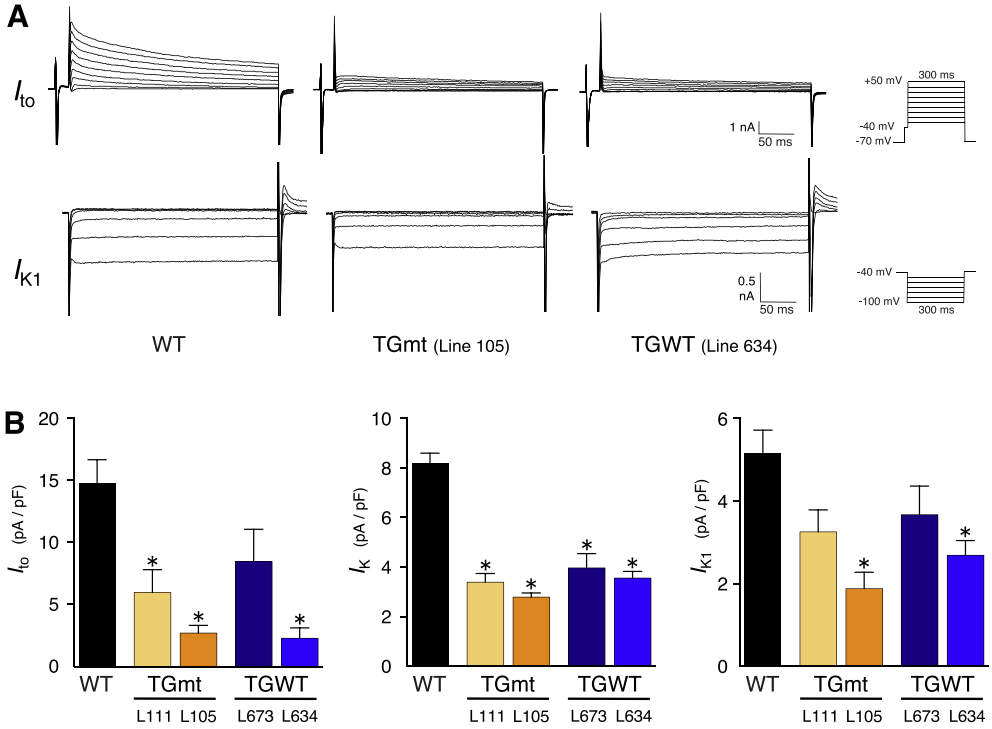

Fig. 3. Voltage-dependent K^+ currents in WT and TG ventricular cells. A: Representative traces of I_{to} and I_{K1} in ventricular myocytes from WT and TG mice. The transient outward current (I_{to}) was measured by delivering 300-ms depolarizing pulses from a holding potential of −70 mV at 0.1 Hz, following a 20-ms prepulse to −40 mV to inactivate Na^+ current, in a solution containing 2 mM $CoCl_2$. The delayed rectifier K^+ current (I_K) and the inward rectifier K^+ current (I_{K1}) were obtained by delivering stepwise depolarization pulses (from −30 mV to +40 mV) and stepwise hyperpolarization pulses (from −50 mV to −100 mV) from a holding potential of −40 mV, respectively. The amplitude of these currents was measured at the end of test pulses. Pulse protocols for these voltage-clamp experiments are shown on the right side. Cardiomyocytes from TGmt and TGWT had lower peaks for I_{to} than that from WT. Furthermore, I_{K1} in TG strains were as well smaller than that in WT. **B:** Summarized data of voltage-dependent K^+ current densities in WT and TG ventricular cells. Current densities are summarized for I_{to} at +50 mV, I_K at +40 mV, and I_{K1} at −60 mV. Overall, TG ventricular cells exhibited less K^+ current densities than that from WT cells. Although there were no significant differences in the I_{to}, I_K, and I_{K1} densities among the four TG lines, Line 673 TG showed comparatively large current density, especially in I_{to} and I_{K1}. Therefore, it may be reasonable that Line 673 (TGWT) has shorter APD and QT/QTc intervals compared with other TG lines. N = 5–21 (cells) in each group. Data are expressed as mean ± SEM. $^*p < 0.05$ vs. WT.

The L-type Ca^{2+} current was also measured. There were no significant differences in the peak Ca^{2+} current density between WT and both TG strains (data not shown).

3.5. Pinacidil-induced K_{ATP} current in ventricular myocytes

Pinacidil-induced K_{ATP} current was recorded using a ramp pulse protocol. Pinacidil at 100 μM successfully increased quasi-steady-state membrane current in ventricular cells from WT and TG mice. As shown in Fig. 4A, the densities of pinacidil-induced outward current in ventricular cells from TG strains were smaller than that in WT ventricular cells. Glibenclamide clearly suppressed the pinacidil-induced K_{ATP} current in these cells. Fig. 4B summarizes K_{ATP} current densities measured at 0 mV following induction by pinacidil (100 μM). The K_{ATP} current density was significantly lower in TG ventricular cells about 40–60% compared with WT cells. There was no significant difference between TG strains (TGmt and TGWT). It was noticeable that pinacidil increased K_{ATP} current in TG cardiomyocyte less than WT cells (Fig. 4C). Collectively, K_{ATP} channels in TG cardiomyocyte were less active than those in WT; furthermore, S422L variant of Kir6.1 (TGmt) did not increase K_{ATP} current compared with TGWT.

3.6. Single K_{ATP} channel analysis

We conducted single channel analysis in the open cell-attached patches to investigate the nature of the K_{ATP} channel in these mouse strains. A trace amount of ATP (1 μM) was added into the basal high K^+ bath solution to decrease the level of channel rundown.[12] Representative single K_{ATP} channel activities are shown in Fig. 5A. In WT cells, K_{ATP} channels were highly active under the control condition with 1 μM ATP, and responded well to an increase of ATP to 100 μM in the bath solution. On the contrary, K_{ATP} channels in TG cardiomyocytes stayed poorly active even under the control condition (1 μM ATP). The calculated open probability at the control condition (NPc) showed that TG strains had significantly lower K_{ATP} channel activities (Fig. 5B). The amplitude of unitary current was measured at the control condition. In open cell-attached patches with pipette potential held at +40 mV, there was no significant difference in the amplitude of unitary current (in pA, WT: 3.42 ± 0.07, TGmt Line 105: 3.33 ± 0.06, and TGWT Line 634: 3.13 ± 0.12, 5–6 cells in each strain), suggesting that conductance of sarcolemmal K_{ATP} channels was similar in these ventricular myocytes.

Further, ATP sensitivity of the channel was analyzed. K_{ATP} channel activities at various ATP concentrations (1–1000 μM) was normalized to that with 1 μM ATP (Fig. 5C). ATP inhibited the K_{ATP} channel activities in a concentration-dependent manner, and 1 mM ATP was enough to repress the K_{ATP} channel activities completely. Although there were significantly large differences between WT and TG strains in the open probabilities at the control condition (NPc) (Fig. 5B), ATP-dependency of the channel inhibition was almost identical between the patches of WT and two TG strains (Fig. 5C). There were no significant differences in IC_{50} value for ATP

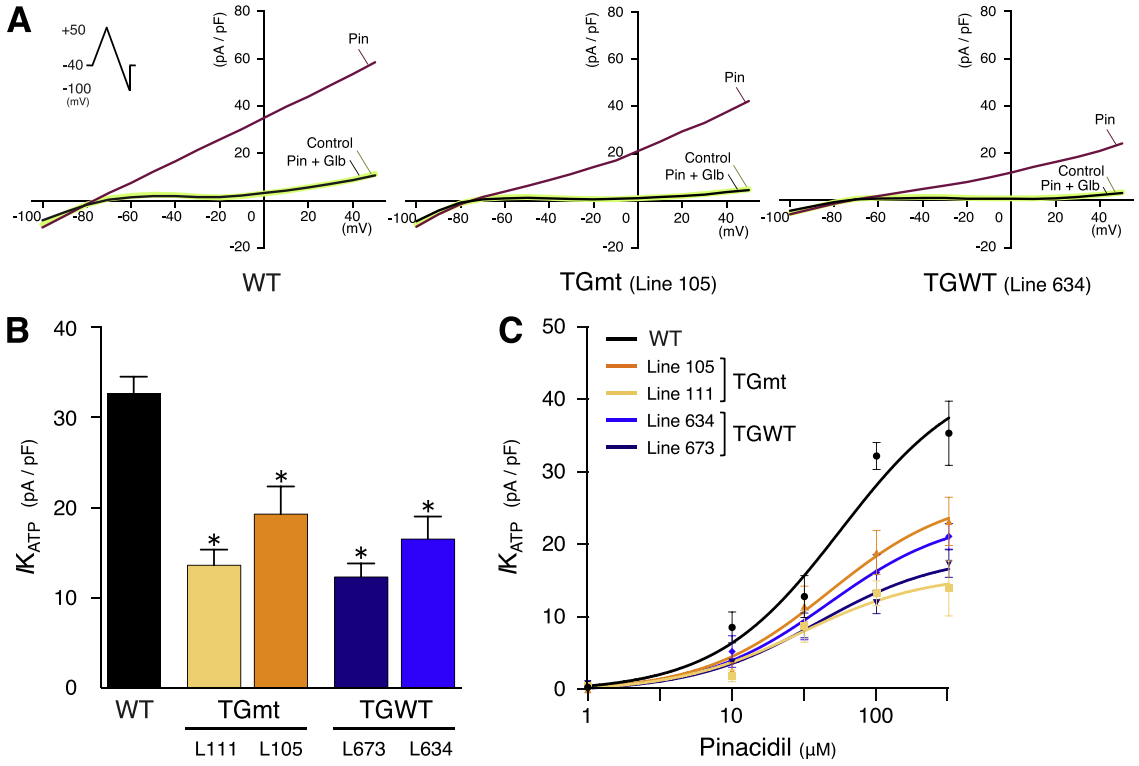

Fig. 4. Pinacidil-induced K_{ATP} current in WT and TG ventricular cells. A: Representative current traces recorded from ventricular cells from TG strains and WT. The quasi-steady-state membrane current was recorded using the ramp pulse protocol (Inset) at an interval of 5 s. The membrane potential was held at −40 mV and depolarized to +50 mV in 300 ms. It was then repolarized or hyperpolarized to −100 mV in 500 ms, during which time the membrane current was automatically plotted against the membrane potential. Although pinacidil (100 μM) definitely induced glibenclamide (10 μM)-sensitive K_{ATP} current in all cases, K_{ATP} currents observed in TGmt and TGWT cells were smaller than that in WT cells. Pin: pinacidil; Glb: glibenclamide. **B:** Pinacidil (100 μM)-induced K_{ATP} current densities at 0 mV in ventricular myocytes. The K_{ATP} current densities in TGmt and TGWT ventricular myocytes were lower by about 40–60% than those from WT cells. There was no significant difference between TG strains (TGmt and TGWT). N = 5–13 (cells) in each group. Data are expressed as mean ± SEM. $^*p < 0.01$ vs. WT. **C:** Concentration response curves for pinacidil-induced K_{ATP} current in ventricular cells from WT and TG strains. Pinacidil-induced K_{ATP} current densities in TG ventricular myocytes were smaller than that from WT cells. In our experimental settings, each cell was exposed to one dose of pinacidil to minimize the effect from the channel rundown. N = 5–18 (cells) in each group. Data are expressed as mean ± SEM.

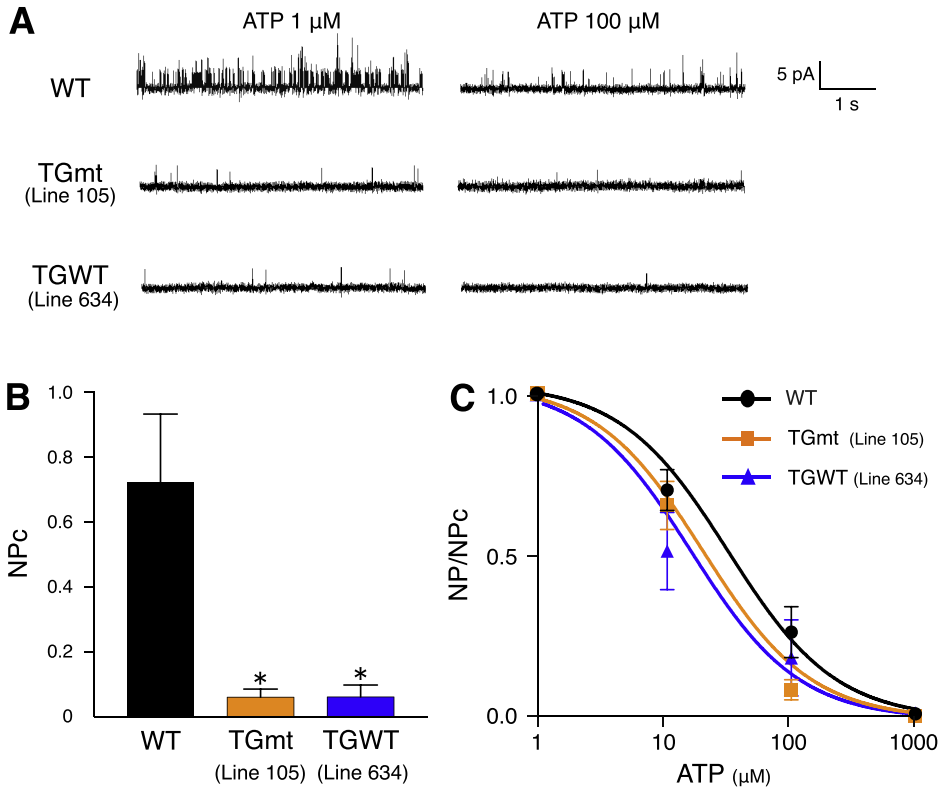

Fig. 5. Single K_{ATP} channel recordings from open cell-attached patches in ventricular cells of WT and TG strains. A: Representative traces of single K_{ATP} channel currents. A trace amount of ATP (1 μM) was added into the basal high K^+ bath solution to decrease the channel rundown. K_{ATP} channels in WT ventricular myocyte were highly active under the control condition (with ATP 1 μM) and responded well to an increase of ATP to 100 μM in the bath solution. In contrast, K_{ATP} channels in TG ventricular myocytes are less active even in the control condition; however, they well responded to an increase in cytosolic ATP. Upward deflections depict the outward K_{ATP} currents from the glass electrode. **B:** Open probability (NPc) of the K_{ATP} channel at the control condition (1 μM ATP). There was no difference between TGmt and TGWT in NPc, although it was significantly higher in WT than Kir6.1 TG strains. N = 5–6 (cells) in each group. Data are expressed as mean ± SEM. $^*p < 0.01$ vs. WT. **C:** Relative open probability (NP/NPc) with varying cytosolic ATP concentrations. Single K_{ATP} channel currents, observed in Kir6.1 TG as well as WT, were all sensitive to ATP to a similar extent. There was no significant difference in IC_{50} value for ATP among the three groups. N = 5–6 (cells) in each group. Data are expressed as mean ± SEM.

among the three groups (mean [95% confidence interval] (μM), WT: 26.8 [18.3–39.2], TGmt Line 105: 16.5 [12.1–22.4], and TGWT Line 634: 12.3 [6.7–22.5], 5–6 cells in each group). Collectively, it was suggested that there were no significant differences between the cardiac K_{ATP} channels of TG and WT animals in the ATP sensitivity and single channel conductance; furthermore, electrophysiological analyses revealed that S422L variant of *KCNJ8* was functionally almost identical to S422 wild type in the transgenic mouse hearts.

4. Discussion

Our *KCNJ8* (Kir6.1) transgenic mice expressing S422L variant (TGmt) and S422 wild type (TGWT) exhibited atypical ECG patterns; however, there were no differences between the variant and wild-type transgenic animals in electrophysiological analyses.

Mouse ECGs normally exhibit "J wave" as a notch after the QRS complex.[14] Both TG mouse strains showed ECG abnormalities characterized by changes of the J-ST segment. The ECG patterns were mostly divided into two patterns; namely "enlarged J wave pattern" and "J-ST segment depression pattern", both of which were associated with marked QT prolongation. There might be a possibility that these changes derived from a non-specific consequence of protein expression under the control of the alpha-MHC promoter. There have been previous demonstrations that non-specific overexpression of protein (e.g. GFP) in the heart leads to a gradual heart failure,[15] and many K^+ currents are down-regulated in such conditions.[16] However, ECG abnormalities shown by our TG mouse strains are not the ones similar to other TG mouse strains.[17,18] This fact supports that ECG abnormalities in our TG model are not the consequence of non-specific overexpression of protein in the heart.

It was revealed that APD_{90} of TG ventricular cells was significantly longer than that of WT cells, explaining the QT prolongation in ECG of TG strains. Furthermore, the voltage-dependent K^+ current (I_{to}, I_K, I_{K1}) densities were down-regulated in ventricular cells of both TG strains, which might be responsible for the APD prolongation and the resultant QT/QTc prolongation. Interestingly, similar phenomenon was reported in another study showing that marked decreases in I_{to} and I_{K1} densities were observed in cardiomyocytes of transgenic mice overexpressing voltage-dependent K^+ channel α-subunit (*KCNQ1*-isoform) although the precise mechanisms remain unclarified.[19]

It has been reported that there are marked regional differences in the densities of voltage-dependent K^+ channels in adult mouse ventricles, which may contribute to ECG waveform.[20] Down-regulation of K^+ currents with different degrees in various parts of TG mouse ventricles might produce atypical ECG changes although we did not investigate the regional differences in the K^+ current densities in this study.

The S422L mutation in the *KCNJ8* gene was first described in association with ERS.[4] In heterologous expression system using cultured cells, K_{ATP} channel assembled with S422L mutant Kir6.1 and SUR2A showed increased current density of K_{ATP} channel compared with that of Kir6.1 wild-type channel, and therefore the gain-of-function mutation of Kir6.1 with the reduced sensitivity (~one-twentieth) to ATP has been lined up as a cause of JWS.[5,6]

Contrary to our expectations, the density of pinacidil-induced K_{ATP} current was lower in ventricular cells of both TG mouse strains compared with that observed in WT ventricular cells in this study. In addition, there was no significant difference in the density of pinacidil-induced K_{ATP} current between TGmt and TGWT ventricular cells. In our single channel patch-clamp experiments, the open probability of K_{ATP} channels was significantly lower in TGmt and TGWT ventricular cells in a control condition. Furthermore, the ATP sensitivity of the K_{ATP} channel in TGmt ventricular cells was almost same with that of the K_{ATP} channel in TGWT ventricular cells. The ATP sensitivity of the K_{ATP} channel in TGmt ventricular cells was not decreased in comparison with that of WT ventricular cells. Thus, the electrophysiological data obtained from TGmt and TGWT mice failed to support the Kir6.1 gain-of-function mutation hypothesis as a direct cause of JWS.

It is still controversial whether the mutation directly associates with JWS. Cooper et al. reported that co-expression of Kir6.1-S422L variant with SUR1 in COS cells did not lead to a gain of K_{ATP} channel function, although another variant form, Kir6.1-C176S, found in a patient with Cantú syndrome, gave rise to enhanced K_{ATP} channel activity with reduced ATP sensitivity when co-expressed with SUR1 or SUR2A.[21] In addition, it has been reported that Kir6.1-S422L allele was found at a higher frequency (~4%) in Ashkenazi Jewish cohort, and there was no evidence showing that they had a predisposition to lethal arrhythmias. Although the ECG recording from a parent who is heterozygote for the S422L mutation presented a subtle J-point elevation, the homozygote son demonstrated no significant ECG abnormalities.[22] Therefore, it would be useful for further deliberative research to be carried out which ensures that the Kir6.1-S422L mutation is a direct cause of JWS.

We previously reported that K_{ATP} channel function in cardiomyocytes was completely blunted in Kir6.2-null mice whereas the channel function was preserved in vascular smooth muscle cells.[12,23] On the other hand, Kir6.1-null mice showed different phenotypes from Kir6.2-null mice; coronary vasospasm resulting in the sudden cardiac death like Prinzmetal angina.[24] Therefore, it has been postulated the functional relevance of Kir6.2 in cardiac K_{ATP} channels, whereas Kir6.1 for vascular K_{ATP} channels.[7] In this context, it is noteworthy that pinacidil-induced K_{ATP} current, as well as APD shortening, can be observed in ventricular cells of Kir6.1-null mice to a similar extent with WT mice.[24] Therefore, it is unlikely that Kir6.1 is dominant in the sarcolemmal K_{ATP} channel function, at least in the mouse heart, although the role of Kir6.1 in cardiomyocytes remains unclear. In the present study, there was no significant difference in the amplitude of unitary K_{ATP} channel current in ventricular cells among WT, TGmt, and TGWT. It was reported that unitary conductance was decreased when K_{ATP} channel was constructed as Kir6.1 or Kir6.1–6.2 tandem co-expressed with SUR2A in a heterologous expression system.[25] These findings also support the concept that Kir6.2 but not Kir6.1 plays an important role in the function of sarcolemmal K_{ATP} channel in the mouse heart. Furthermore, Kir6.1-S422L mutation could not affect sarcolemmal K_{ATP} channel function since we could not find any differences between TGmt and TGWT at single channel level.

We analyzed the gene expression levels of Kir6.2, SUR1 and SUR2 in ventricular tissues of WT, TGmt and TGWT mice. The mRNA expression levels of Kir6.2 and SUR2 tended to be decreased in the TGmt and TGWT ventricles when compared with those in WT ventricle (data not shown). These findings may partly explain the decreased activity of Kir6.2-assembled K_{ATP} channel although the precise mechanism(s) remain unclarified.

In conclusion, electrophysiological analyses of *KCNJ8* transgenic mice did not substantiate the S422L mutation in *KCNJ8* gene as a direct cause of JWS although atypical ECG changes were observed in these TG mice.

Conflicts of interest

None to be declared.

Acknowledgements

The authors are grateful to Mses. Y. Reien and T. Tachibana for their technical assistance.

References

1. Haïssaguerre M, Derval N, Sacher F, et al. Sudden cardiac arrest associated with early repolarization. *N Engl J Med*. 2008;358:2016–2023.
2. Antzelevitch C. Genetic, molecular and cellular mechanisms underlying the J wave syndromes. *Circ J*. 2012;76:1054–1065.
3. Antzelevitch C, Yan GX, Ackerman MJ, et al. J-Wave syndromes expert consensus conference report: emerging concepts and gaps in knowledge. *Heart Rhythm*. 2016;13:e295–324.
4. Haïssaguerre M, Chatel S, Sacher F, et al. Ventricular fibrillation with prominent early repolarization associated with a rare variant of KCNJ8/K_{ATP} channel. *J Cardiovasc Electrophysiol*. 2009;20:93–98.
5. Barajas-Martínez H, Hu D, Ferrer T, et al. Molecular genetic and functional association of Brugada and early repolarization syndromes with S422L missense mutation in *KCNJ8*. *Heart Rhythm*. 2012;9:548–555.
6. Medeiros-Domingo A, Tan BH, Crotti L, et al. Gain-of-function mutation S422L in the *KCNJ8*-encoded cardiac K_{ATP} channel Kir6.1 as a pathogenic substrate for J-wave syndromes. *Heart Rhythm*. 2010;7:1466–1471.
7. Seino S, Miki T. Physiological and pathophysiological roles of ATP-sensitive K^+ channels. *Prog Biophys Mol Biol*. 2003;81:133–176.
8. Gulick J, Subramaniam A, Neumann J, Robbins J. Isolation and characterization of the mouse cardiac myosin heavy chain genes. *J Biol Chem*. 1991;266:9180–9185.
9. Inagaki N, Tsuura Y, Namba N, et al. Cloning and functional characterization of a novel ATP-sensitive potassium channel ubiquitously expressed in rat tissues, including pancreatic islets, pituitary, skeletal muscle, and heart. *J Biol Chem*. 1995;270:5691–5694.
10. Matsumoto A, Yamafuji M, Tachibana T, Nakabeppu Y, Noda M, Nakaya H. Oral 'hydrogen water' induces neuroprotective ghrelin secretion in mice. *Sci Rep*. 2013;3:3273.
11. Kojima A, Matsumoto A, Nishida H, et al. A protective role of Nox1/NADPH oxidase in a mouse model with hypoxia-induced bradycardia. *J Pharmacol Sci*. 2015;127:370–376.
12. Suzuki M, Li RA, Miki T, et al. Functional roles of cardiac and vascular ATP-sensitive potassium channels clarified by Kir6.2-knockout mice. *Circ Res*. 2001;88:570–577.
13. Lusis AJ, Yu J, Wang SS. The problem of passenger genes in transgenic mice. *Arterioscler Thromb Vasc Biol*. 2007;27:2100–2103.
14. Boukens BJ, Rivaud MR, Rentschler S, Coronel R. Misinterpretation of the mouse ECG: 'musing the waves of *Mus musculus*'. *J Physiol*. 2014;592:4613–4626.
15. Huang WY, Aramburu J, Douglas PS, Izumo S. Transgenic expression of green fluorescence protein can cause dilated cardiomyopathy. *Nat Med*. 2000;6:482–483.
16. Nabauer M, Kaab S. Potassium channel down-regulation in heart failure. *Cardiovasc Res*. 1998;37:324–334.
17. Li J, McLerie M, Lopatin AN. Transgenic upregulation of I_{K1} in the mouse heart leads to multiple abnormalities of cardiac excitability. *Am J Physiol Heart Circ Physiol*. 2004;287:H2790–H2802.
18. Lottonen-Raikaslehto L, Rissanen R, Gurzeler E, et al. Left ventricular remodeling leads to heart failure in mice with cardiac-specific overexpression of VEGF-B_{167}: echocardiography and magnetic resonance imaging study. *Physiol Rep*. 2017;5. http://dx.doi.org/10.14814/phy2.13096.
19. Demolombe S, Lande G, Charpentier F, et al. Transgenic mice overexpressing human KvLQT1 dominant-negative isoform. Part I: phenotypic characterisation. *Cardiovasc Res*. 2001;50:314–327.
20. Brunet S, Aimond F, Li H, et al. Heterogeneous expression of repolarizing, voltage-gated K^+ currents in adult mouse ventricles. *J Physiol*. 2004;559:103–120.
21. Cooper PE, Reutter H, Woelfle J, et al. Cantú syndrome resulting from activating mutation in the *KCNJ8* gene. *Hum Mutat*. 2014;35:809–813.
22. Veeramah KR, Karafet TM, Wolf D, Samson RA, Hammer MF. The *KCNJ8*-S422L variant previously associated with J-wave syndromes is found at an increased frequency in Ashkenazi Jews. *Eur J Hum Genet*. 2014;22:94–98.
23. Suzuki M, Sasaki N, Miki T, et al. Role of sarcolemmal K_{ATP} channels in cardioprotection against ischemia/reperfusion injury in mice. *J Clin Invest*. 2002;109:509–516.
24. Miki T, Suzuki M, Shibasaki T, et al. Mouse model of Prinzmetal angina by disruption of the inward rectifier Kir6.1. *Nat Med*. 2002;8:466–472.
25. Kono Y, Horie M, Takano M, et al. The properties of the Kir6.1–6.2 tandem channel co-expressed with SUR2A. *Pflügers Arch*. 2000;440:692–698.